Heliyon 9 (2023) e16570

Contents lists available at ScienceDirect

Heliyon

journal homepage: www.cell.com/heliyon

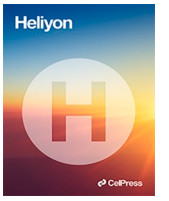

Research article

Bifurcation analysis on ion sound and Langmuir solitary waves solutions to the stochastic models with multiplicative noises

Fahad Sameer Alshammari [a,*], Harun-Or- Roshid [b,**], Md Asif [b], Md Fazlul Hoque [b,c], Abdullah Aldurayhim [a]

[a] Department of Mathematics, College of Science and Humanities in Alkharj, Prince Sattam bin Abdulaziz University, Alkharj, 11942, Saudi Arabia
[b] Department of Mathematics, Pabna University of Science and Technology, Bangladesh
[c] Faculty of Nuclear Sciences and Physical Engineering, Czech Technical University, Brehova 7, 115 19 1, Czech Republic

ARTICLE INFO

Keywords:
Bifurcation
Ion sound and Langmuir wave
Stochastic model
Multiplicative noise

ABSTRACT

This article explores on a stochastic couple models of ion sound as well as Langmuir surges propagation involving multiplicative noises. We concentrate on the analytical stochastic solutions including the travelling and solitary waves by using the planner dynamical systematic approach. To apply the method, First effort is to convert the system of equations into the ordinary differential form and present it in form of a dynamic structure. Next analyze the nature of the critical points of the system and obtain the phase portraits on various conditions of the corresponding parameters. The analytic solutions of the system in an account of distinct energy states for each phase orbit are performed. We also show how the results are highly effective and interesting to realize their exciting physical as well as the geometrical phenomena based on the demonstration of the stochastic system involving ion sound as well as Langmuir surges. Descriptions of effectiveness of the multiplicative noise on the obtained solutions of the model, and its corresponding figures are demonstrated numerically.

1. Introduction

Unpredictability and fluctuations have recently been a much more interesting research area in the context of wave phenomena in nature. Reducing arbitrary fluctuations of waves and signals played a significant role in the fields of electromagnetic theory, signal processing, biological behaviors as neutral agents, finance system, oceanography nonlinear optic and many engineering applications [1–5]. The models, which reflect the random fluctuations with times, are mostly connected to the stochastic differential systems [6,7]. Most of such systems are high frequencies and have unique characteristics in the form of ion sound wave with random amplitudes that occurs under the action of ponder-motive force. Thus, it is one attractive attention to study ion noise as well as Langmuir solitonic surges amid to their different behaviors. Due to this purpose, we concentrate our attention on the system of stochastic dynamical models for the ion noise in addition Langmuir surges [8,9] including multiple racket during Ito logic. The stochastic dynamical couple models (SDCMs) of ion noise together with Langmuir surges is given by,

* Corresponding author.
** Corresponding author.
E-mail addresses: f.alshammari@psau.edu.sa (F.S. Alshammari), harunorroshidmd@gmail.com (H.-O. Roshid).

https://doi.org/10.1016/j.heliyon.2023.e16570
Received 19 October 2022; Received in revised form 16 May 2023; Accepted 19 May 2023
Available online 23 May 2023

$$\begin{aligned} &F_{tt} - F_{xx} - 2\left(|G|^2\right)_{xx} = 0 \\ &iG_t + \frac{1}{2}G_{xx} - GF = i\kappa G\varepsilon_t \end{aligned} \tag{1}$$

where $F(x,t)$ and $Ge^{iw_p t}$, κ and $\varepsilon(t)$ as sign the normalized density perturbation and electric region to the Langmuir wavering, sound potency and the usual Wiener progression, respectively. We assume that the racket is an invariable throughout the overall space. One dimensional model for Langmuir instability has been derived in Ref. [8], which coincides to the model (1) treated as $\kappa = 0$. Langmuir solitons and various types of solutions of distinct nature have been done [9–12]. In fact, the weak Langmuir turbulence was also investigated by Musher [9], and Langmuir collapsed under pumping with energy dissipation was done by Degtiarev et al. [10]. Two- and three-dimensional Langmuir collapse systems have been numerically studied by Dyachenko et al. [11] and Zakharov et al. [12] respectively. Yajima et al. [13] was formed solitonic interaction solutions of the Sonic-Langmuir wave model with ion-acoustic waves through the inverse scattering approach. However, there are huge new techniques to derive various exact dynamical solutions to the nonlinear complex models literally, in particular, the Jacobi elliptic function expansion [14], the Improved Kudryashov [15], the modified simple equation [16], the variational iteration [17], the modified piecewise variational iteration [18], the tan ($\varphi/2$)-expansion [19], the Riccati-Bernoulli sub-ODE function [20], the Petrov-Kudrin-Xiong [21], the first integral method [22], the finite difference [23], the $\exp(-\varphi(\eta))$-expansion [24], the Hirota bilinear [25–27], the sumudu homotopy perturbation [28], Adomian's decomposition [29], the (G'/G)-expansion [30,31], the unified [32,33] and the bifurcation scheme with theory of dynamic systems approach [34,35], which have been effectively employed to obtain new travelling brandish solutions of complex nonlinear precise models. Among these methods, the bifurcation as well as theory of dynamic structures approach are one most qualitative as this can derive the exact solutions according to the energy orbits of their phase portraits. Besides, stochastic soliton of stochastic nonlinear models are highly investigated by recent young scientists [36–39] to reducing arbitrary fluctuations of wave's amplitudes. It is still unexplored the stochastic wave solution following each energy orbits of phase portraits from Hamiltonian of the model.

Thus, we sport light on the stochastic model (1) to establish more new dynamical stochastic solutions including the travelling and solitary wave solutions according to each energy orbit for various phase portraits depending on distinct parametric conditions of the mode by using the planner dynamical systematic approach. The analytic solutions of the system would like to achieve and illustrate graphically with impact of noise.

2. The ODE structure of the model

Due to obtain travelling surges of SDCM Eq. (1), we first utilize the subsequent complex renovation,

$$G(x,t) = v(\xi)e^{\left(i\Phi + \kappa\varepsilon(t) - \kappa^2 t\right)}, \xi = wx + st \text{ and } \Phi = px + ht, \tag{2}$$

where p, h, s, w are nonzero constants and v is a deterministic function.

Plugging Eq. (2) together with its various derivatives into the second equation of (1), we attain to (real part only)

$$\frac{1}{2}w^2 v'' - \left(\frac{1}{2}p^2 + hv\right) - vF = 0. \tag{3}$$

We now take the advantage of $F(x,t) = U(\xi), \xi = wx + st$, it leads to

$$F_{tt} = s^2 U'', F_{xx} = w^2 U''. \tag{4}$$

Inserting now Eq. (4) into the first equation of (1) reaches to

$$\left(s^2 - w^2\right)U'' - 2w^2\left(v^2\right)'' e^{2\kappa\varepsilon(t) - 2\kappa^2 t} = 0. \tag{5}$$

Taking expectation on both sides, we obtain

$$\left(s^2 - w^2\right)U'' - 2w^2\left(v^2\right)'' E e^{2\kappa\varepsilon(t)} = 0, \tag{6}$$

here U as well as v are functions to be resolved later. As $\varepsilon(t)$ is the typical usual random function, we can choose $E(e^{\delta\varepsilon(t)}) = e^{\frac{\delta^2}{2}t}$ for any real invariable δ into Eq. (6), which yields

$$\left(s^2 - w^2\right)U'' - 2w^2\left(v^2\right)'' = 0. \tag{7}$$

After two times integration regards to ξ, Eq. (7) reduces to

$$\left(s^2 - w^2\right)U - 2w^2 v^2 = b_1\xi + b_2, \tag{8}$$

where b_1 and b_2 are constants of integration. Here we settle $b_1 = b_2 = 0$ into Eq. (8) transpire to

$$U = \frac{2w^2 v^2}{s^2 - w^2}. \tag{9}$$

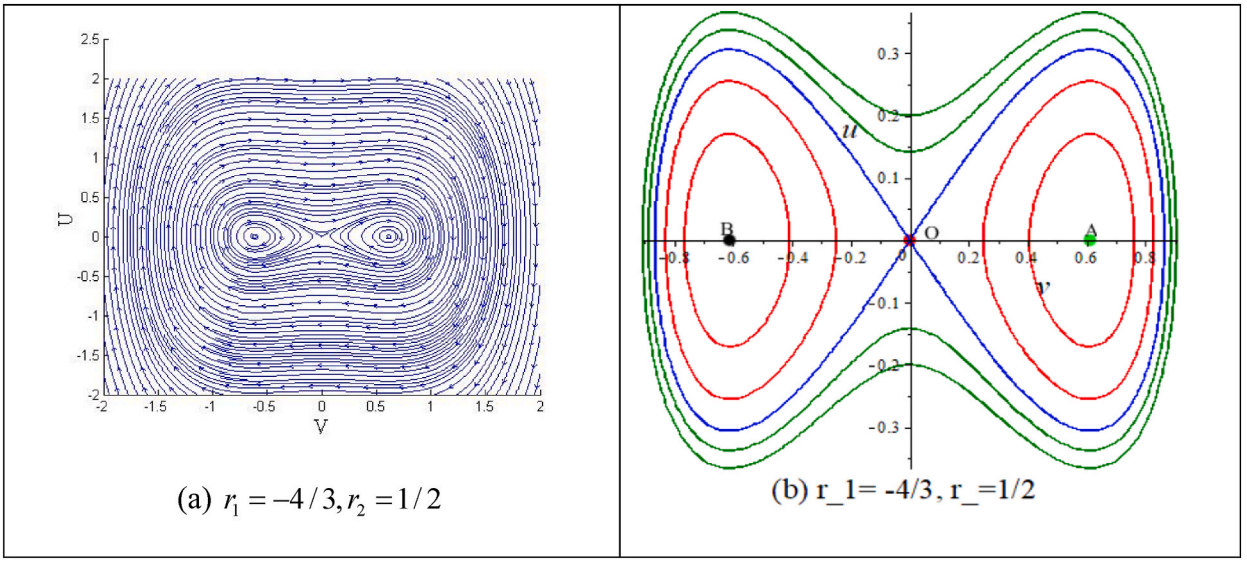

Fig-1. (a) Stream flows with directions and (b) Phase orbits for $r_1 < 0, r_2 > 0$.

Utilizing Eq. (9) into Eq. (8), yields a second order ODE form as

$$v'' - r_1 v^3 - r_2 v = 0, \tag{10}$$

where $r_1 = \frac{4}{s^2 - w^2}$ and $r_2 = \frac{p^2 + 2h}{w^2}$.

3. Bifurcation analysis of the model with phase portrait

The model (10) can be rewritten in a dynamical system form as follows,

$$\begin{aligned} v' &= u \\ u' &= r_1 v^3 + r_2 v \end{aligned}. \tag{11}$$

It is shown that system (11) has critical points $O(0,0)$, $A\left(\sqrt{-\frac{r_2}{r_1}}, 0\right), B\left(-\sqrt{-\frac{r_2}{r_1}}, 0\right)$ and also has a first integral form with the Hamiltonian

$$\mathrm{H}(v,u) = \frac{u^2}{2} - \frac{r_1}{4}v^4 - \frac{r_2}{2}v^2. \tag{12}$$

Determination of Jacobian matrices at the equilibrium points are:

$$\det J_O = -r_2, \det J_A = 2r_2 \text{ and } \det J_B = 2r_2.$$

If $\frac{r_2}{r_1} < 0$, the system has three-equilibrium points O, A, B and arises here two cases:

(i) For $r_2 > 0$ implies O-saddle. A, B–centers; there exists two homoclinic orbits Γ^A and Γ^B that connected at the saddle O. The centers are encircled by a family of periodic orbits as

$$\Gamma^A(h) = \left\{ H(v,u) = h, h \in \left(\frac{r_2^2}{4r_1}, 0\right) \right\} \text{ and } \Gamma^B(h) = \left\{ H(v,u) = h, h \in \left(\frac{r_2^2}{4r_1}, 0\right) \right\}$$

(ii) For $r_2 < 0$ implies O-center, A, B are saddles. The center is encircled by a family of periodic orbits as $\Gamma^O(h) = \left\{ H(v,u) = h, h \in \left(0, \frac{r_2^2}{4r_1}\right) \right\}$.

On the other parametric condition as $\frac{r_2}{r_1} > 0$, the system has only one real equilibrium points at O.

(i) For $r_2 > 0$, implies O-saddle and (ii) For $r_2 < 0$, implies O-center.

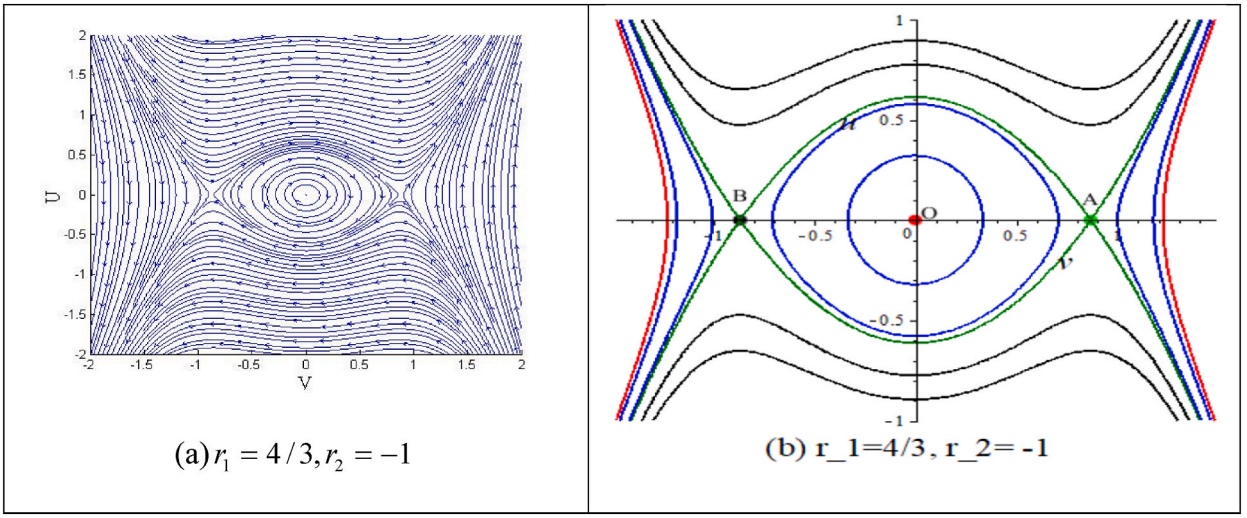

Fig-2. **(a)** Stream flows with directions and (b) Phase orbits for $r_1 > 0, r_2 < 0$.

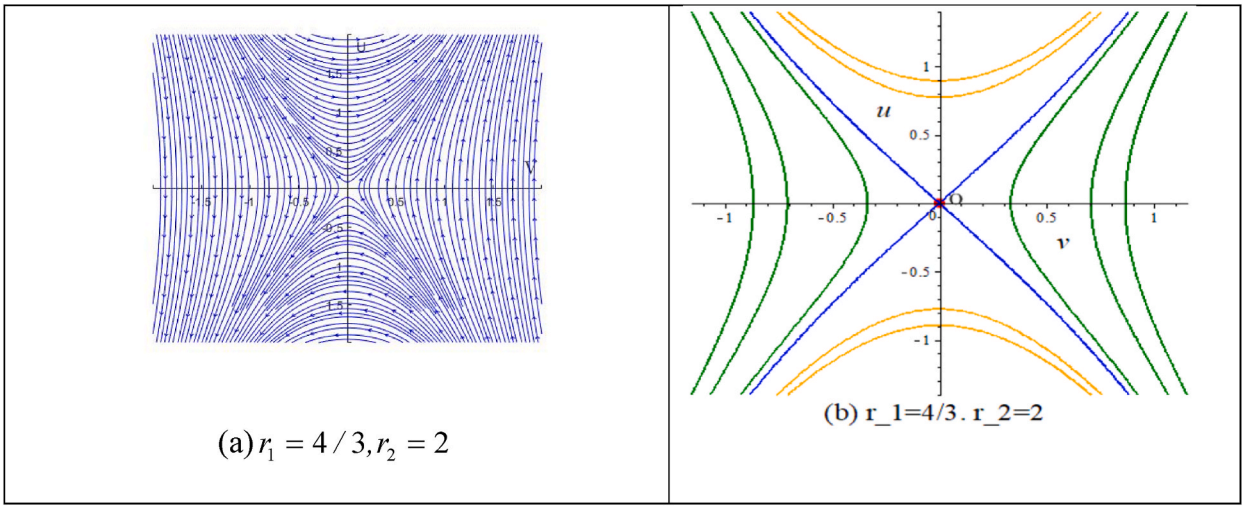

Fig-3. **(a)** Stream flows with directions and (b) Phase orbits for $r_1 > 0, r_2 > 0$.

Thus, four cases arise depending on the values of r_1, r_2 such as
Case1: $r_1 < 0, r_2 > 0$, **Case2:** $r_1 > 0, r_2 < 0$, **Case3:** $r_1 > 0, r_2 > 0$ and **Case4:** $r_1 < 0, r_2 < 0$.

Case-1. If $s = 1, w = 2, p = 2, h = -1$, then $r_1 = -\frac{4}{3}$ and $r_2 = \frac{1}{2}$ provides the streamlines and phase portrait in Fig-1.

Case-2. If $s = 2, w = 1, p = 1, h = -1$, then $r_1 = \frac{4}{3}$ and $r_2 = -1$ which provides the streamlines and phase portrait in Fig-2.

Case-3. If $s = 2, w = 1, p = 2, h = -1$, then $r_1 = \frac{4}{3}$ and $r_2 = 2$ which provides the streamlines and phase portrait in Fig-3.

Case-4. If $s = 1, w = 2, p = 1, h = -1$, then $r_1 = -\frac{4}{3}$ and $r_2 = -\frac{1}{4}$ that provides the streamlines and phase portrait in Fig-4.

4. Solitary and travelling wave solutions

Suppose that the stochastic model has a continuous solution $v(\xi)$, $\xi \in R$ and $\lim_{\xi \to \infty} v(\xi) = u_1$, $\lim_{\xi \to -\infty} v(\xi) = u_2$. If $u_1 = u_2$, the result $v(\xi)$ is a solitary wave, as, it is a kink (anti-kink) wave result. It is recognized that the bell types solitary, kink (anti-kink) even cyclic wave solutions occur, respectively, for homoclinic, hetero-clinic and periodic orbits of the phase portraits. The perfect parametric presentation for the bounded orbit of $v(\xi)$ can be illustrated by the exact travelling wave solutions of (11). We utilize the Hamiltonian (12) to construct such solutions with the first equation of (11), which yields

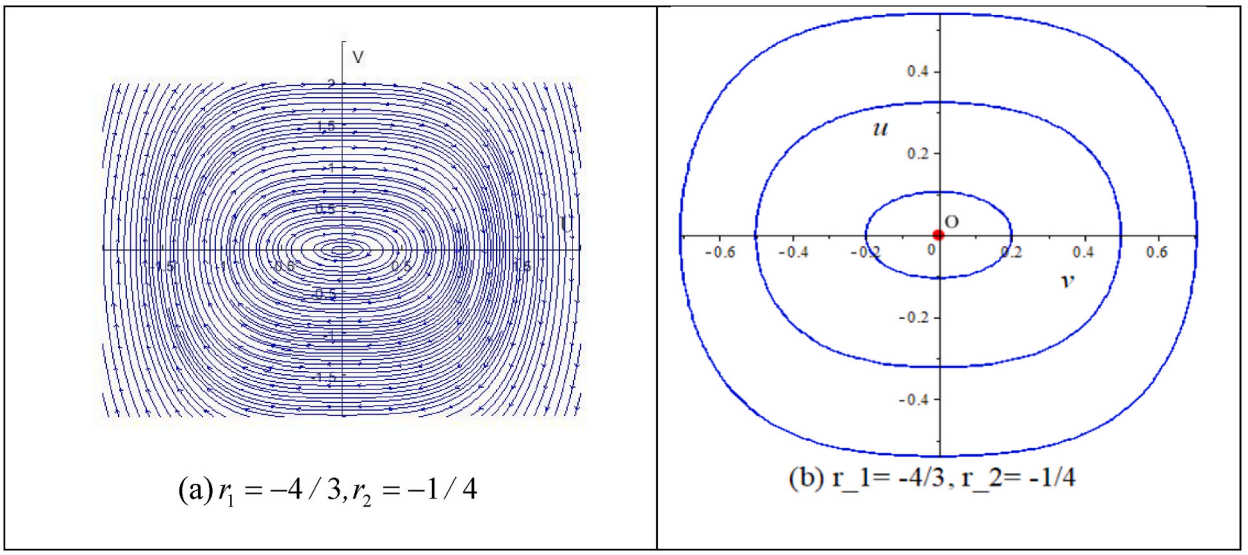

Fig-4. (a) Stream flows with directions and (b) Phase orbits for $r_1 < 0, r_2 < 0$.

$$\int \frac{dv}{\sqrt{2}\sqrt{\mathrm{K}_4(v)}} = \int d\xi, \tag{13}$$

where $\mathrm{K}_4(v) = h + \frac{r_1}{4}v^4 + \frac{r_2}{2}v^2$ in v..

Depending on the values of r_1, r_2 and on a certain level of energy h, we can evaluate the integral of Eq. (13) and construct a wave solution for Eq. (1). The total energies or Hamiltonian values at the critical points are $H_O = 0, H_A = \frac{{r_2}^2}{4r_1}$ and $H_B = \frac{{r_2}^2}{4r_1}$. According to these results, we obtain various families of wave solutions as follows:

Family-1: In the Fig-1, there are three types of orbits for dynamical system (11) and these orbits are identified by $\mathrm{H}(u, v) = h$ for dissimilar energy states h as $h > 0, h = 0, h \in ..$

• For the energy level $h > 0$, a family of orbits cut the v-axis $(v = 0)$ at two points, as identified by green coloured curves in Fig-1(b). As a result, the polynomial (13) has two real and two complex conjugate zeros, presented by $k_4(v) = \frac{-r_1}{4}({v_1}^2 - v^2)({v_2}^2 + v^2)$. After integration of Eq. (13), and using the transformation Eq. (2): $G(x,t) = v(\xi)e^{(i\Phi + \kappa\varepsilon(t) - \kappa^2 t)}, \xi = wx + st, \Phi = px + ht$, we get the required result

$$G(x,t) = \frac{v_2}{\sqrt{{v_1}^2 + {v_2}^2}} \times \frac{cn\left[\sqrt{\frac{-r_1}{2}({v_1}^2 + {v_2}^2)}\ (\xi + a), \frac{-v_2}{\sqrt{({v_1}^2 + {v_2}^2)}}\right]}{dn^2\left[\sqrt{\frac{-r_1}{2}({v_1}^2 + {v_2}^2)}\ (\xi + a), \frac{-v_2}{\sqrt{({v_1}^2 + {v_2}^2)}}\right]} e^{(i\Phi + \kappa\varepsilon(t) - \kappa^2 t)}. \tag{14}$$

It is shown that the travelling wave solution (14) is periodic with periodic $4\sqrt{\frac{2}{-r_1}}\,k\left(\frac{-v_1}{\sqrt{{v_1}^2 + {v_2}^2}}\right)$, where $\mathrm{K}(k)$ is a Jacobi elliptic integral of the first type.

• For energy level zero $h = 0$, the orbits are passing through the origin (a saddle point) and returns to it again, as demonstrated by blue coloured curves in Fig-1(b). It is homoclinic orbit that can refer habitually to the continuation of bell type solitary wave. Such orbit cuts the v-axis $(u = 0)$ in three points presented by $K_4(v) = \frac{r_1}{4}v^2\left(v^2 + \frac{2r_2}{r_1}\right)$. Corresponding result after integration and using Eq. (2), yields

$$G(x,t) = \pm\sqrt{-\frac{2r_2}{r_1}}\sec h\left\{-\sqrt{r_2}(\xi + a)\right\}e^{(i\Phi + \kappa\varepsilon(t) - \kappa^2 t)}, \tag{15}$$

where $\xi = wx + st, \Phi = px + ht$.

• For the level energy in the interval $h \in$, equation $\mathrm{H}(u, v) = h$ defines periodic orbits around the two equilibrium points A, B. Every orbit of this family cuts the v-axis $(u = 0)$ in four points identified by red-coloured circles in Fig-1(b), and so it can be written as $\mathrm{K}_4(v) = \frac{r_1}{4}({v_1}^2 - v^2)({v_2}^2 - v^2)$. The periodic travelling wave solution for this case can be expressed as

$$G(x,t) = \pm v_2 sn\left[\sqrt{\frac{-r_1}{2}}(\xi + a), \frac{v_2}{v_1}\right]e^{(i\Phi + \kappa\varepsilon(t) - \kappa^2 t)}. \tag{16}$$

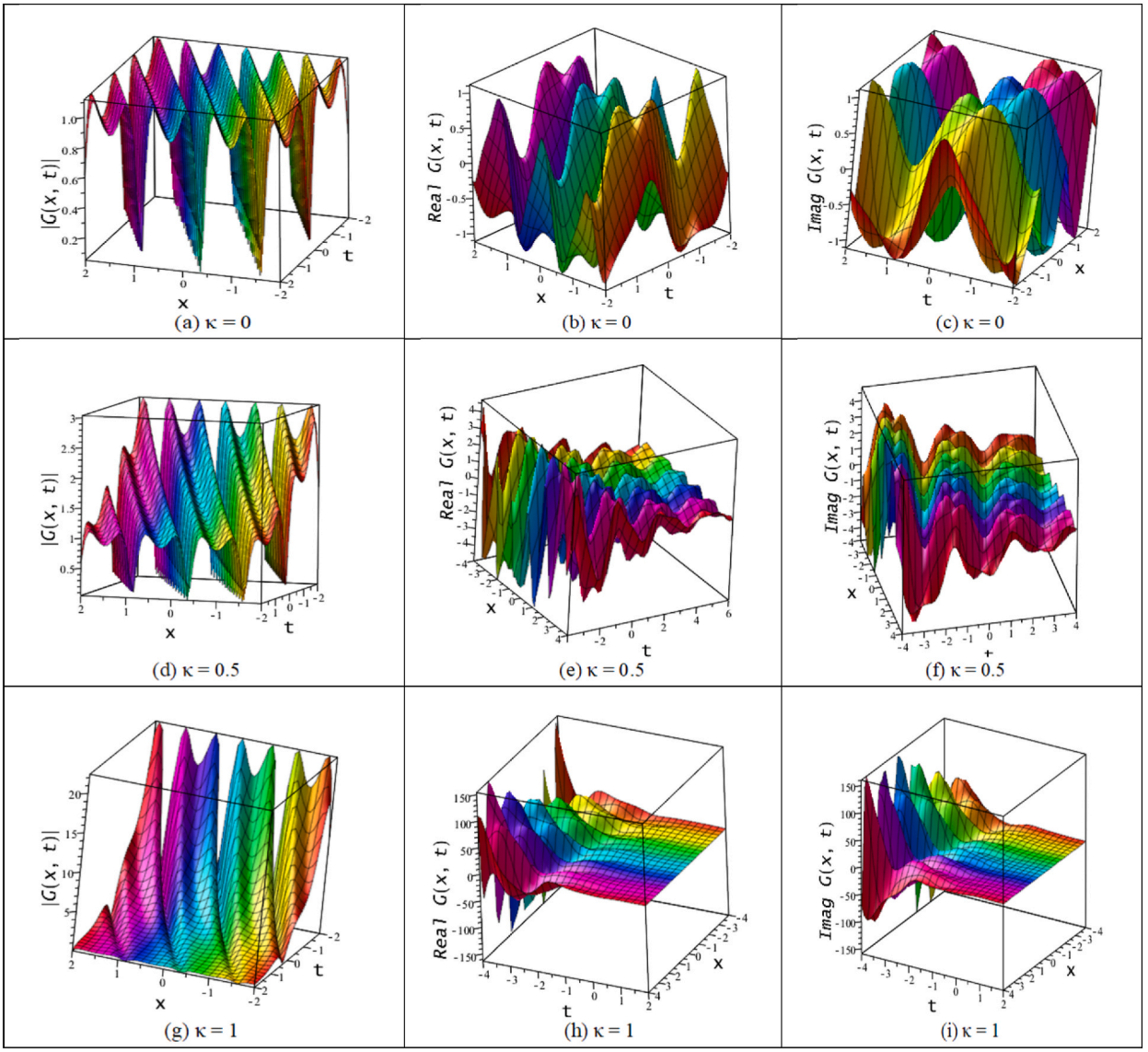

Fig-5. Periodic wave solution of Eq. (14) for the parameters $s = 1, w = 2, p = 2, h = -1, a = 0$: (a) absolute, (b) real part, (c) imaginary part for $\kappa = 0$; (d) absolute, (e) real part, (f) imaginary part for $\kappa = 0.5$; (g) absolute, (h) real part, (i) imaginary part for $\kappa = 1$..

Family-2: Following the Fig-2, there are four types of orbits for the dynamical system (11) and these orbits are identified via $H(u, v) = h$ for dissimilar energy states h as either $h = \frac{r_2^2}{4r_1}$ *or* $h = 0$ *or* $h > \frac{r_2^2}{4r_1}$ *or* $0 < h < \frac{r_2^2}{4r_1}$.

• For the energy level $h = \frac{r_2^2}{4r_1}$, the existing family of orbits connects two saddle points described by $H(v, u) = \frac{r_2^2}{4r_1}$. The describing orbits are indicated by green coloured curves in Fig-2(b). Every orbit of this family cuts the v-axis $(u = 0)$ at two points. Thus the expression (13) has two recurred real zeros and takes the structure $k_4(v) = \frac{r_1}{4}\left(v^2 + \frac{r_2}{r_1}\right)^2$. The corresponding result after integration and using Eq. (2), yields the explicit depiction of the kink wave solution

$$G(x,t) = \pm\sqrt{\frac{-r_2}{r_1}}\tanh\sqrt{\frac{-r_2}{2}}(\xi + a)e^{\left(i\Phi + \kappa\varepsilon(t) - \kappa^2 t\right)}. \tag{17}$$

• For the energy level $h = 0$, a family of orbits existed there are sketched in Fig-2(b) in red color. Every orbit of this family does not cut the u-axis $(v = 0)$. The expression (13) interprets by $k_4(v) = \frac{-r_1}{4}v^2\left(v^2 + \frac{2r_2}{r_1}\right)$, which admits the subsequent wave solution with Eq. (2) is

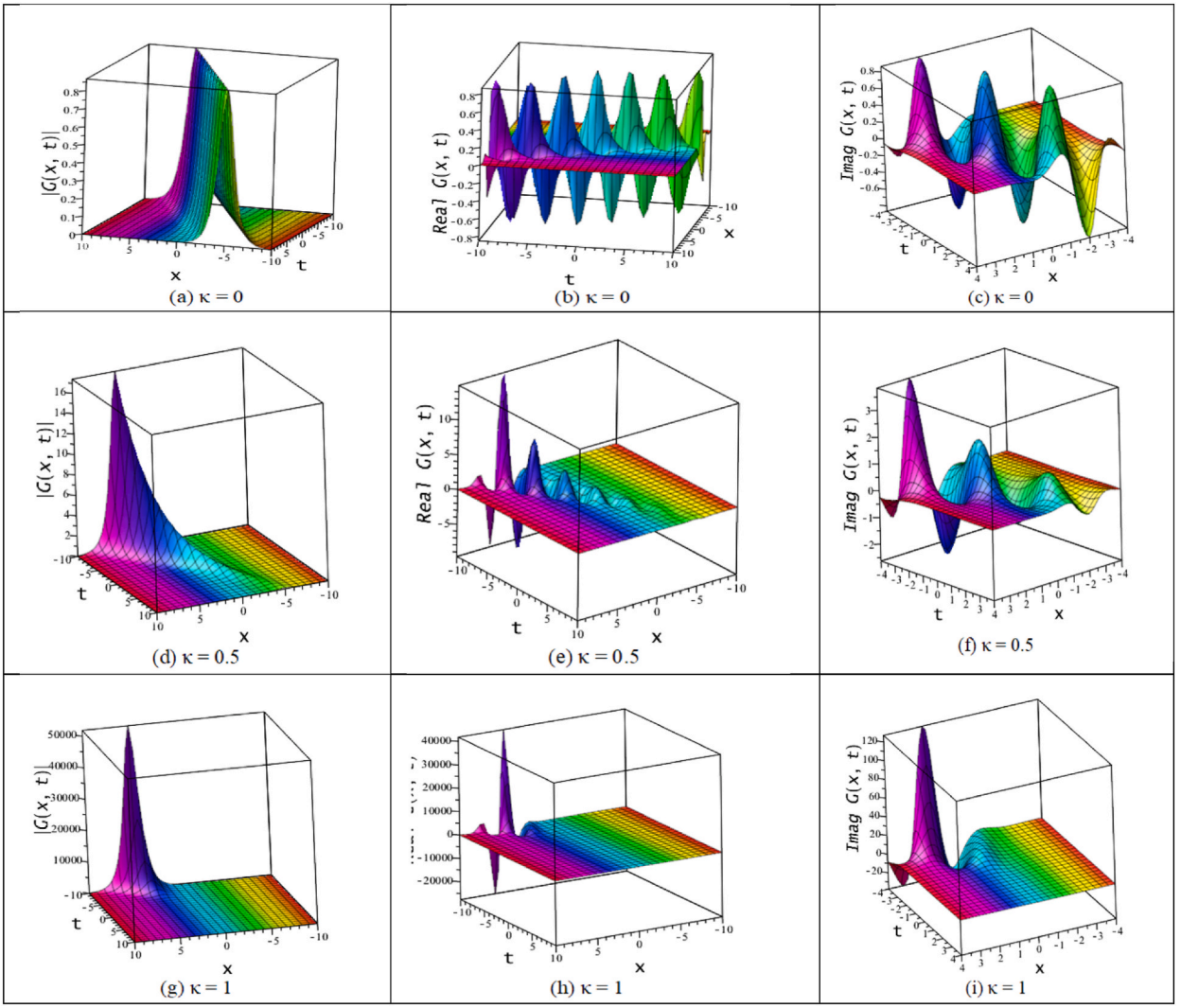

Fig-6. Periodic wave solution of Eq. (15) for the parameters $s = 1, w = 2, p = 2, h = -1$: (a) absolute, (b) real part, (c) imaginary part for $\kappa = 0$; (d) absolute, (e) real part, (f) imaginary part for $\kappa = 0.5$; (g) absolute, (h) real part, (i) imaginary part for $\kappa = 1$..

$$G(x,t) = \sqrt{\frac{-2r_2}{r_1}}\sec\sqrt{-r_2}(\xi + a)e^{\left(i\Phi + \kappa\varepsilon(t) - \kappa^2 t\right)}. \tag{18}$$

• For the energy level, $h > \frac{r_2^2}{4r_1}$, a family of orbits exists indicating a black coloured curve in Fig-2(b). These orbits never cut the v-axis ($u = 0$), and have complex roots only as $k_4(v) = \frac{r_1}{4}(v^2 + {v_1}^2)(v^2 + {v_2}^2)$, where $v_{2,3}^2 = g + il$. After integration of Eq. (13) and using Eq. (2), we acquire a travelling wave solution in form

$$G(x,t) = \sqrt{\frac{g^2 + l^2}{il - g}}sn\left[\sqrt{\frac{r_1(g - il)}{2}}(\xi + a), \frac{g + il}{\sqrt{g^2 + l^2}}\right]e^{\left(i\Phi + \kappa\varepsilon(t) - \kappa^2 t\right)}. \tag{19}$$

• For the energy level in the interval $0 < h < \frac{r_2^2}{4r_1}$, a family of periodic orbits existed encircling the origin. Such a family is described by $H(v,u) = h$ indicate by blue-coloured curves in Fig-2(b). Every orbit of such family cuts the v-axis ($u = 0$) at four points can be expressed via $k_4(v) = \frac{r_1}{4}(v^2 - {v_1}^2)(v^2 - {v_2}^2)$. After integration with the expression and utilizing Eq. (2) provides an explicit travelling wave solution

$$G(x,t) = v_2 sn\left[\sqrt{\frac{r_1}{2}}(\xi + a), \frac{v_2}{v_1}\right]e^{\left(i\Phi + \kappa\varepsilon(t) - \kappa^2 t\right)}. \tag{20}$$

Family-3: Following Fig-3(b), there are three families of orbits designed for dissimilar values and restrictions on h. The explicit

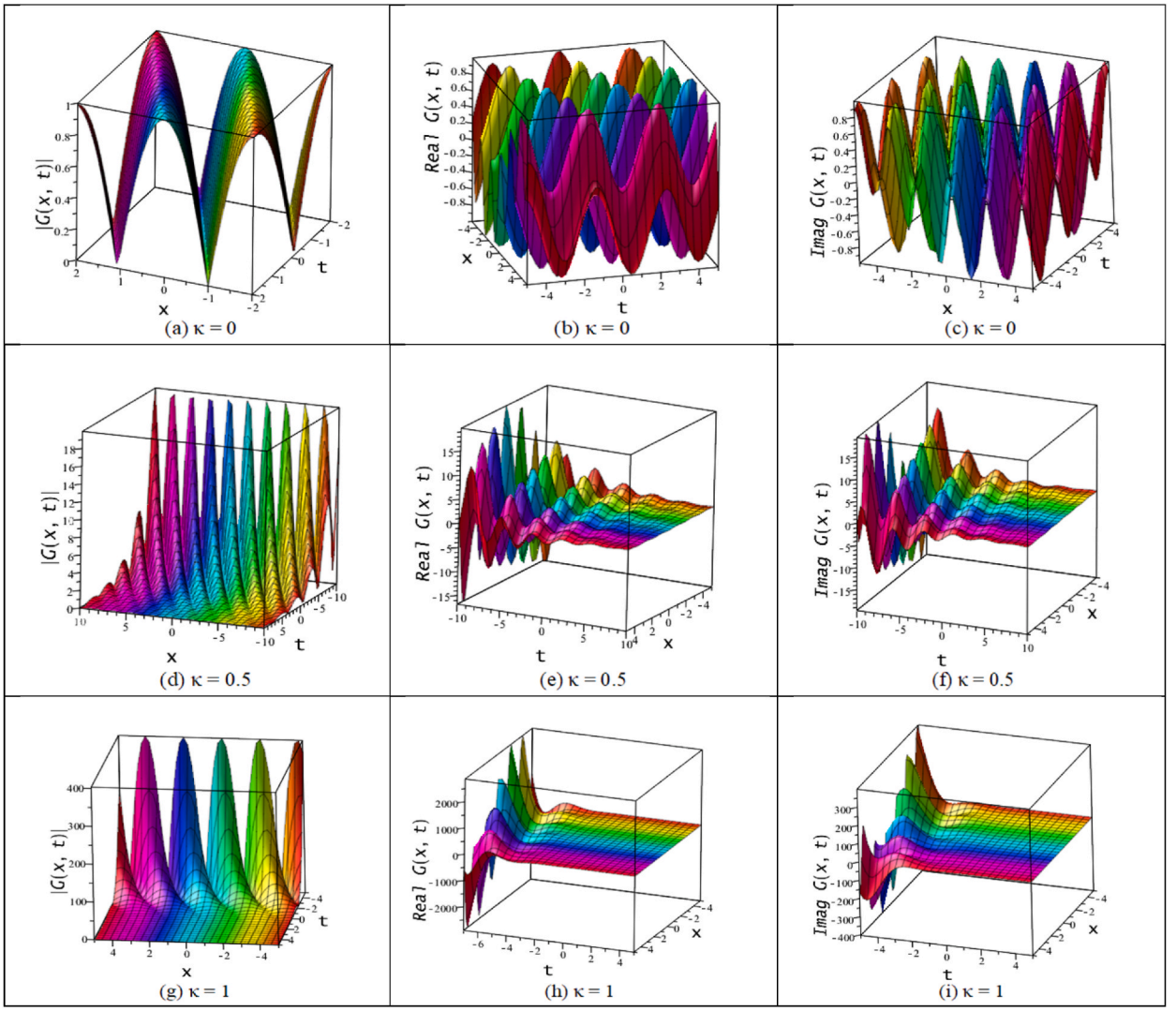

Fig-7. Periodic wave solution of Eq. (16) for the parameters $s = 1, w = 2, p = 2, h = -1, a = 0$: (a) absolute, (b) real part, (c) imaginary part for $\kappa = 0$; (d) absolute, (e) real part, (f) imaginary part for $\kappa = 0.5$; (g) absolute, (h) real part, (i) imaginary part for $\kappa = 1$..

depiction for wave solution of system (11) is established through the polynomial (13) for distinct parametric values of h as follows:

• For the level of energy zero ($h = 0$), a family of orbits passes through the origin indicated by blue-coloured curves in Fig-3(b). This family can be expressed via the polynomial (13) $k_4(v) = \frac{r_1}{4}v^2\left(v^2 + \frac{2r_2}{r_1}\right)$ only, whose integration with Eq. (2) gives

$$G(x,t) = \mp\sqrt{\frac{2r_2}{r_1}}\csc h\sqrt{r_2}(\xi + a)e^{\left(i\Phi + \kappa\varepsilon(t) - \kappa^2 t\right)}, \tag{21}$$

where a is an integral constant.

• For a positive energy level $h > 0$, a family of orbits appears here marked with golden colour in Fig-3(b). These orbits never intersect the v-axis ($u = 0$) and such orbits can be expressed by a polynomial (13), which contains no real zeroes, i.e. $k_4(v) = \frac{r_1}{4}({v_1}^2 + v^2)({v_2}^2 + v^2)$. Its integral value together with Eq. (2), gives the result

$$G(x,t) = -v_1\frac{sn\left[v_2\sqrt{\frac{r_1}{2}}(\xi + a), \sqrt{1 - \frac{{v_1}^2}{{v_2}^2}}\right]}{cn\left[v_2\sqrt{\frac{r_1}{2}}(\xi + a), \sqrt{1 - \frac{{v_1}^2}{{v_2}^2}}\right]}e^{\left(i\Phi + \kappa\varepsilon(t) - \kappa^2 t\right)}, \tag{22}$$

where $sn(v,k), cn(v,k)$ and $dn(v,k)$ are the Jacobi elliptic function.

• For a negative energy level $h < 0$, the Hamiltonian (12) has a family of orbits marked with green colour in Fig-3(b). Such orbits

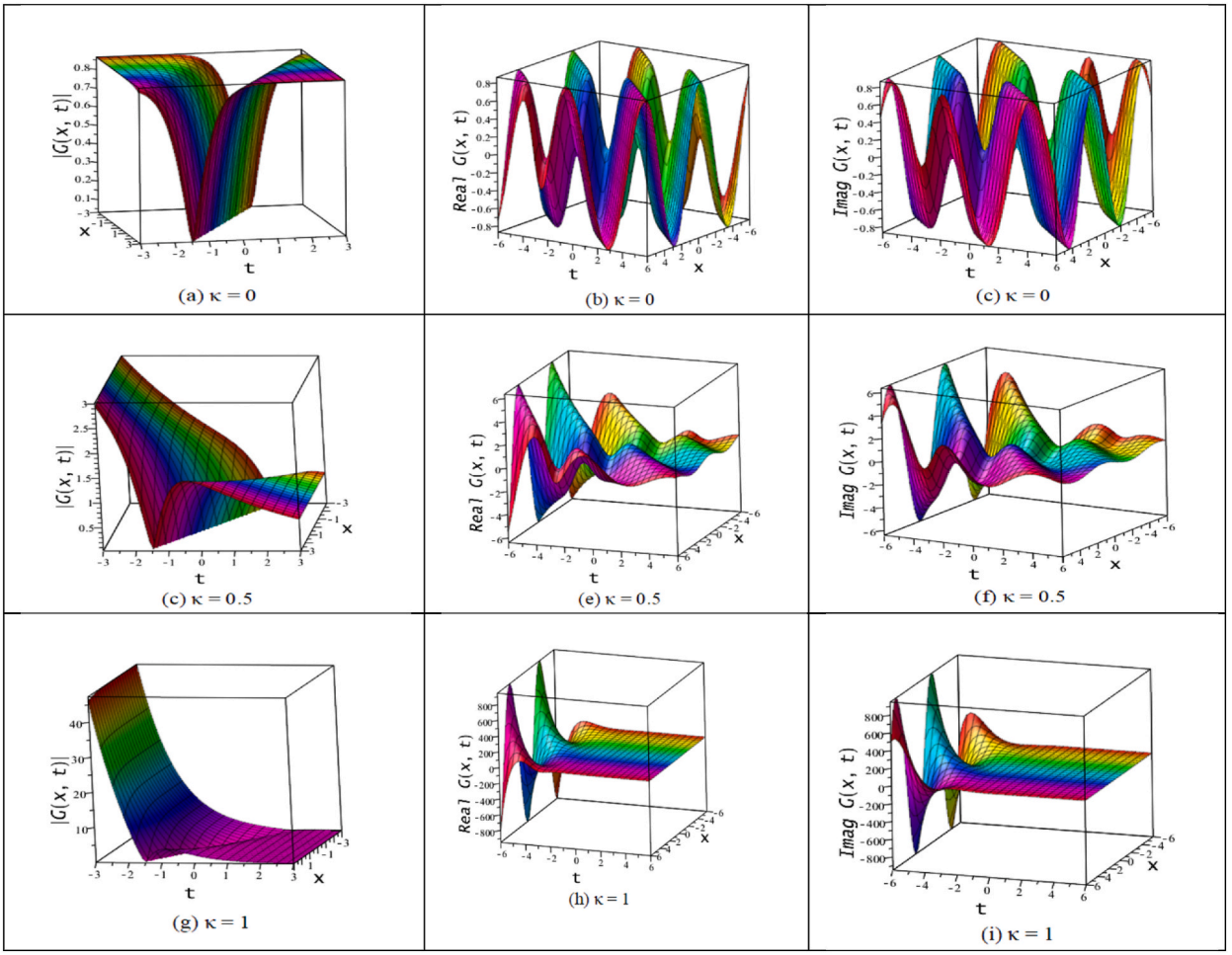

Fig-8. Periodic wave solution of Eq. (17) for the parameters $s = 2, w = 1, p = 1, h = -1$: (a) absolute, (b) real part, (c) imaginary part for $\kappa = 0$; (d) absolute, (e) real part, (f) imaginary part for $\kappa = 0.5$; (g) absolute, (h) real part, (i) imaginary part for $\kappa = 1$..

cut at the two points of v-axis and can be described by the polynomial $k_4(v) = \frac{r_1}{4}(v^2 - {v_1}^2)({v_2}^2 + v^2)$ which has a pair of complex conjugate zeros. After integration of (13) with $k_4(v) = \frac{r_1}{4}(v^2 - {v_1}^2)({v_2}^2 + v^2)$ and utilizing Eq. (2), yields

$$G(x,t) = \frac{cn\left[\sqrt{\frac{r_1}{2}({v_1}^2 + {v_2}^2)}\,(\xi + a), \frac{v_2}{\sqrt{({v_1}^2 + {v_2}^2)}}\right]}{dn^2\left[\sqrt{\frac{r_1}{2}({v_1}^2 + {v_2}^2)}\,(\xi + a), \frac{v_2}{\sqrt{({v_1}^2 + {v_2}^2)}}\right]} e^{\left(i\Phi + \kappa\varepsilon(t) - \kappa^2 t\right)}. \tag{23}$$

Family-4: This case has one real critical point at the origin as a center only. Thus a family of periodic orbits arises enclosing the origin, showed in the Fig-4(b). Such family of orbits presented by the curves identified through $H(v,u) = h$, where $h > 0$. Nature of the Fig-4(b) indicates that every orbit of such family cuts the v- axis $(u = 0)$ at two points and can be presented by $k_4(v) = \frac{-r_1}{4}({v_1}^2 - v^2)({v_2}^2 + v^2)$, where $v_1 = \sqrt{\frac{-4h}{r_1}}$. Now, integral values of Eq. (13) with this $k_4(v)$ together with Eq. (2), leads to

$$v = \pm\frac{v_1}{\sqrt{2}} sn\left[v_1\sqrt{\frac{-r_1}{2}}(\xi + a), \frac{-1}{\sqrt{2}}\right] e^{\left(i\Phi + \kappa\varepsilon(t) - \kappa^2 t\right)}. \tag{24}$$

5. Comparison, interpretations and impact of noise on the wave propagation

This study is devoted to highlighting the wave behaviors and the effect of noise on the ion sound wave solutions of model (1), which was studied through He's semi-inverse, the Riccati–Bernoulli sub-ODE and the sine–cosine techniques by Mohammad et al. [38]. They used only auxiliary schemes to find stochastic solutions, but we derived solution following energy orbits from Hamilatonian of the model. All of our solutions are satisfying dynamical nature of phase portraits. How the action of a nonlinear force in which a charged

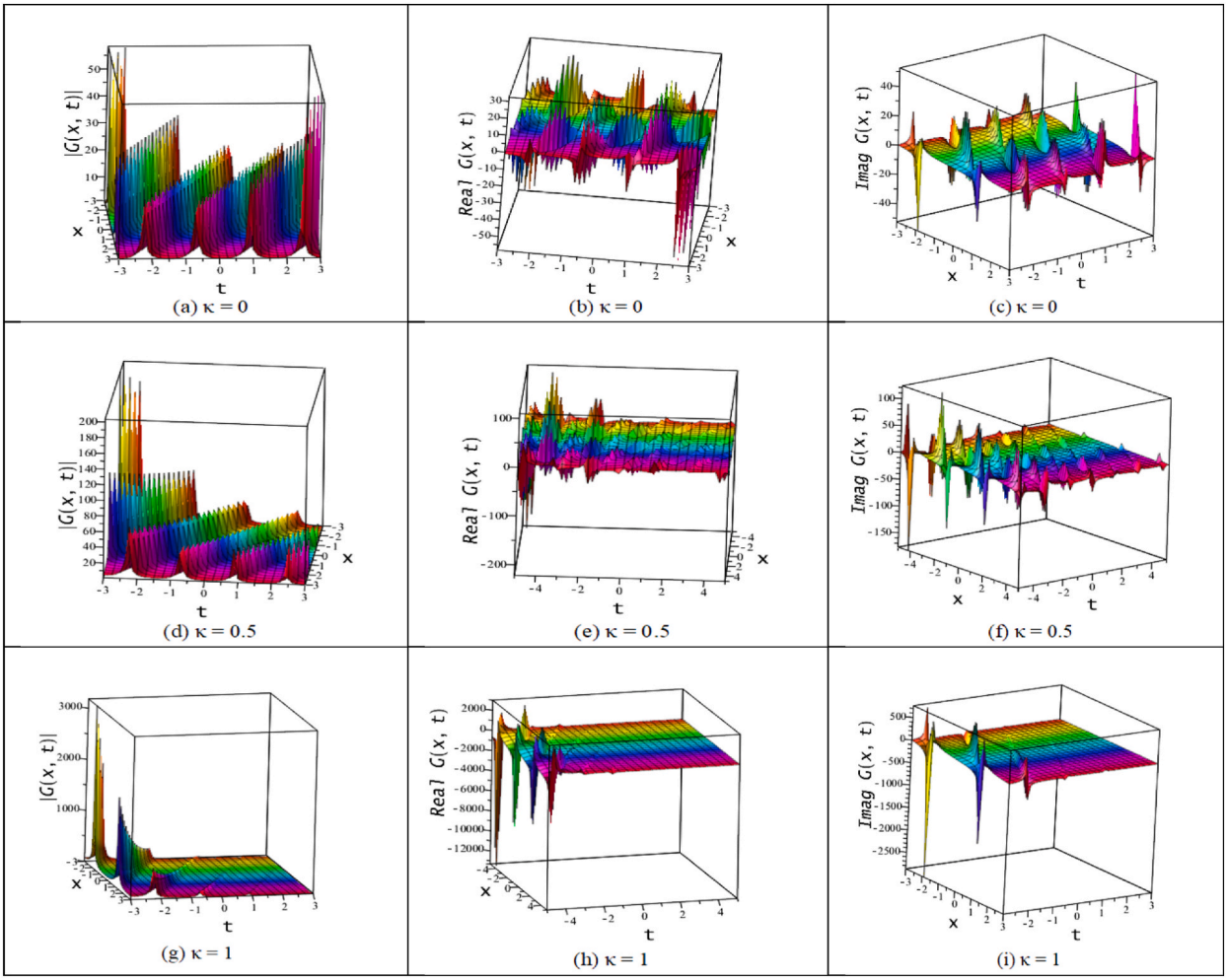

Fig-9. Periodic wave solution of Eq. (18) for the parameters $s = 2, w = 1, p = 1, h = -1$: (a) absolute, (b) real part, (c) imaginary part for $\kappa = 0$; (d) absolute, (e) real part, (f) imaginary part for $\kappa = 0.5$; (g) absolute, (h) real part, (i) imaginary part for $\kappa = 1$..

element acquires an observation in an inhomogeneous fluctuating electro-magnetic ground owing to elevated amplitude also. Indeed, the model acts as many crucial cases to illustrate the high-frequency Langmuir oscillation with rising noise. The phase orbits and solutions according to each energy orbit have been constructed by the planner dynamical theory of the SDCM model. The achieved results and their physical structures will help us to visualize dynamical characteristics and their sensitivity to different initial conditions as well. It can significantly change the qualitative activities and effects of novel characters. The solutions are addressed to illustrate the numerical structures in the following descriptions.

The stochastic solutions (14), (16), (19), (20), (22), (23), and (24) appear in terms of Jacobi elliptic functions that exhibit periodic behaviors with oscillations. Among the results, Eqs. 14 and 23 are supper periodic waves; (16), (20), (24) are periodic waves; and (18), (19), and (22) are singular periodic waves. The nature of the solutions (14), (16) and (18) are illustrated only in Fig-5, Fig-7 and Fig-9 respectively. Besides these, we achieve stochastic soliton solutions that seem in the hyperbolic function form such as (15), (17) and (21). The solutions (15) and (17) are also graphically displayed in Fig-6 and Fig-8 whose natures are respectively the Bright and Dark bells, while properties of result (21) is a singular bell soliton. The dark as well as bright solitons transmit thru nonlinear dispersive medium and these solitons designate solitary waves with lesser and larger peak intensity respectively. We are predominantly attracted to the impact of noise acting on wave transmission as it is an indispensable problematic in plasma, electromagnetic fields and nonlinear optics. In this research, we also show the configurations of each result by changing the stochastic coefficients $\kappa = 0, 0.5, 1$. It is shown that the amplitude of any travelling waves remains the same as $\kappa = 0$ always though time increases. It is evident from the figures that for the increases of the value of the coefficients the higher amplitudes wave gradually goes to diminish with oscillation as times increase and ultimately diminished as $t \to \infty$..

6. Conclusions

The stochastic models of ion noise as well as Langmuir surges amid multiple rackets are considered here due to present their significant applications in the high frequency charged electric field. We investigated the bifurcation analysis of the nonlinear model through a planer dynamical scheme. All possible phase portraits are found owing to various conditions on the involved parameters. We derived analytic nonlinear wave solutions of the model according to each energy orbit of all phase portraits. As a result, we achieved stochastic Dark and Bright bell soliton solutions as well as stochastic super periodic and periodic wave solutions. Due to the effects of the noise term, we observed that Langmuir oscillation arising on the wave profile and the amplitude of the oscillating wave gradually going down to diminish as time goes on. The wave amplitude is going to diminish as quickly as they increase in racket strength. Finally, graphical illustrations are provided to show the effect of parameters on the obtained wave solutions. It is evident that the planer dynamical approach is much more suitable as it provides all possible results following each orbit of the phase portraits. In near future, one can find interaction of stochastic solitons and chaotic chaos dynamics of the same model, which is not stated here.

Funding

This study is supported via funding from Prince Sattam bin Abdulaziz University project number (PSAU/2023/R/1444).

Author contributions statement

Fahad Sameer Alshammari conceived and designed the experiments. Harun-Or-Roshid performed the experiments; analyzed and interpreted the data. Md. Asif performed the experiments; analyzed and interpreted the data; wrote the paper. Md Fazlul Hoque contributed reagents, materials, analysis tools or data; analyzed and interpreted the data. Abdullah Aldurayhim analyzed and interpreted the data.

Data availability statement

No data was used for the research described in the article.

Declaration of competing interest

The authors declare the following financial interests/personal relationships which may be considered as potential competing interests: Harun-Or-Roshid, Pabna University of Science & Technology, Pabna-6600, Bangladesh. Reports administrative support, equipment, drugs, or supplies, and statistical analysis were provided by Pabna University of Science and Technology, Bangladesh. Harun-Or-Roshid reports a relationship with Pabna University of Science and Technology that includes: employment and non-financial support. Fahad Sameer Alshammari has patent with royalties paid to Prince Sattam bin Abdulaziz University, Alkharj 11942, Saudi Arabia. Authors declared that they have no any financial interest and conflict among them.

Acknowledgements

The authors grateful to the Prince Sattam bin Abdulaziz University, Alkharj 11942, Saudi Arabia for their financial supports that help us in the quality research and presentation of this paper.

References

[1] M. Eslami, Soliton-like solutions for the coupled Schrödinger's-Boussinesq equation, Opt. Int. J. Light Electron Opt. 126 (2016) 3987–3991.
[2] M.A.E. Abdelrahman, S.Z. Hassan, M. Inc, The coupled nonlinear Schrödinger-type equations, Mod. Phys. Lett. 34 (2020), 2050078.
[3] Y. Shi, M. Pana, D. Peng, Replicator dynamics and evolutionary game of social tolerance: the role of neutral agents, Econ. Lett. 159 (2017) 10–14.
[4] S. Liu, Q. Zhou, A. Biswas, W. Liu, Phase-shift controlling of three solitons in dispersion-decreasing fibers, Nonlinear Dynam. 98 (2019) 395–401.
[5] W.W. Mohammed, M.A.E. Abdelrahman, M. Inc, A.E. Hamza, M.A. Akinlar, Soliton solutions for system of ion sound and Langmuir waves, Opt. Quant. Electron. 52 (2020) 460.
[6] M.A.E. Abdelrahman, W.W. Mohammed, The impact of multiplicative noise on the solution of the Chiral nonlinear Schrödinger equation, Phys. Scripta 95 (2020), 085222.
[7] S. Albosaily, W.W. Mohammed, M.A. Aiyashi, M.A.E. Abdelrahman, Exact solutions of the (2+1)-dimensional stochastic Chiral nonlinear schrodinger equation, Symmetry 12 (2020) 1874.
[8] V.E. Zakharov, A.N. Pushkarev An, R.Z. Sagdeev, et al., Throughout" modelling of the one-dimensional Langmuir turbulence, Sov. Phys. Dokl. 34 (1989) 248–251.
[9] S.L. Musher, A.M. Rubenchik, V.E. Zakharov, Weak Langmuir turbulence, Phys. Rep. 252 (1995) 178–274.
[10] L.M. Degtiarev V.E. Zakharov, R.Z. Sagdeev, et al., Langmuir collapse under pumping and wave energy dissipation, Sov. Phys. JETP 58 (1983) 710–715.
[11] A.I. Dyachenko, V.E. Zakharov, A.M. Rubenchik, et al., Numerical simulation of two-dimensional Langmuir collapse, Sov. Phys. JETP 67 (1988) 513–518.
[12] V.E. Zakharov, A.N. Pushkarev, A.M. Rubenchik, et al., Numerical simulation of three-dimensional Langmuir collapse in plasma, Pis'ma v Zh. Eksp. Teor. Fiz. 47 (1988) 287–290.
[13] N.Y. Yajima, M.O. Oikawa, Formation and interaction of Sonic–Langmuir solitons: inverse scattering method, Prog. Theor. Phys. 56 (1976) 1719–1739.
[14] Y. Xiao, H. Xue, H. Zhang, A new extended Jacobi elliptic function expansion method and its application to the generalized shallow water wave equation, Journal of Appl. Math., 2012 (2012), 896748, https://doi.org/10.1155/2012/896748, 21.
[15] Z. Rahman, M.Z. Ali, H.O. Roshid, Closed form soliton solutions of three nonlinear fractional models through a proposed Improved Kudryashov method, Chin. Phys. B 30 (2021), 050202.

[16] M.M. Roshid, H.O. Roshid, Exact and explicit traveling wave solutions to two nonlinear evolution equations which describe incompressible viscoelastic Kelvin-Voigt fluid, Heliyon 4 (2018), https://doi.org/10.1016/j.heliyon.2018.
[17] E. Yusufoglu, The variational iteration method for studying the Klein-Gordon equation, Appl. Math. Lett. 21 (2008) 669–674.
[18] M.G. Sakar, F.A. Erdogan, A Modified Piecewise Variational Iteration Method for Solving a Neutral Functional-Differential Equation with Proportional Delays, IECMSA-2013, 2nd International Eurasian Conference On Mathematical Sciences and Applications, 2013. Aug 26–29; SarajevoBosnia and Herzegovina.
[19] M.F. Hoque, H.O. Roshid, Optical soliton solutions of the Biswas-Arshed model by the expansion approach, Phys. Scripta 95 (2020), 075219.
[20] X.F. Yang, Z.C. Deng, Y. Wei, A Riccati-Bernoulli sub-ODE method for nonlinear partial differential equations and its application, Adv. Differ. Equ. 1 (2015) 117–133.
[21] E.Y. Petrov, A.V. Kudrin, Exact axisymmetric solutions of the Maxwell equations in a nonlinear non-dispersive medium, Phys. Rev. Lett. 104 (2010), 190404.
[22] G. Akram, N. Mahak, Application of the first integral method for solving (1+1) Dimensional Cubic-Quintic Complex Ginzburg-Landau equation, Optik 164 (2018) 210, https://doi.org/10.1016/j.ijleo.2018.02.108.
[23] F. Erdogan, M.G. Sakar, A Finite Difference Method on Layer-Adapted Mesh for Singularly Perturbed Delay Differential Equations, 3rd International Eurasian Conference on Mathematical Sciences and Applications, 2014 Aug 25–28 (Vienna-Austria).
[24] H.O. Roshid, M.A. Rahman, The $\exp(-\varphi(\eta))$-expansion method with application in the $(1+1)$-dimensional classical Boussinesq equations, Res. Phys. 4 (2014) 150–155.
[25] Z. Rahman, M.Z. Ali, H.O. Roshid, M.S. Ullah, X.Y. Wen, Dynamical structures of interaction wave solutions for the two extended higher-order KdV equations, Pramana - J. Phys. 95 (3) (2021) 134, https://doi.org/10.1007/s12043-021-02155-4.
[26] H.O. Roshid, M.S. Khatun, N.F.M. Noor, H.M. Baskonus, F.B.M. Belgacem, Breather, multi-shock waves and localized excitation structure solutions to the Extended BKP–Boussinesq equation, Commun. Nonlinear Sci. Numer. Simul. 101 (2021), 105867.
[27] F.S. Alshammari, R.S. Albilasi, M.F. Hoque, H.O. Roshid, Overtaking collisions of m-shock waves and interactions of n $(n\to\infty)$-lump, m $(m\to\infty)$-solitons, τ $(\tau\to\infty)$-periodic waves solutions to a generalized (2+1)-dimensional new KdV model, Chin. J. Phys. 80 (2022) 385–396.
[28] A. Atangana, Extension of the Sumudu homotopy perturbation method to an attractor for one dimensional Keller–Segel equations, Appl. Math. Model. 39 (2015) 2909–2916.
[29] J.F. Cheng, Y.M. Chu, Solution to the linear fractional differential equation using Adomian Decomposition method, Math. Probls. Engineer. (2011), 587068, https://doi.org/10.1155/2011/587068, 2011.
[30] W.W. Mohammed, M. Alesemi, S. Albosaily, N. Iqbal, M. El-Morshedy, The exact solutions of stochastic fractional-space Kuramoto-Sivashinsky equation by using (G'/G)-expansion method, Mathematics 9 (2021) 2712.
[31] A.A.N. Stéphane, D. Augustin, M.B. César, Extended (G'/G) method applied to the modified nonlinear Schrodinger equation in the case of ocean rogue waves, J. Mar. Sci. 4 (2014) 246–256, https://doi.org/10.4236/ojms.2014.44023.
[32] M.S. Ullah, H.O. Roshid, M.Z. Ali, A. Biswas, M. Ekici, S. Khan, L. Moraru, A.K. Alzahrani, M.R. Belic, Optical soliton polarization with Lakshamanan-Porsezian Daniel model by unified approach, Results Phys. 22 (2021), 103958.
[33] S. Akcagil, T. Aydemir, A new application of the unified method, NTMSCI 6 (1) (2018) 185–199, https://doi.org/10.20852/ntmsci.2018.261.
[34] H. Bin, L. Jibin, L. Yao, R. Weiguo, Bifurcations of travelling wave solutions for a variant of Camassa-Holm equation, Nonlinear Anal. R. World Appl. 9 (2) (2008) 222–232.
[35] Y. Zhou, Q. Liu, Kink Waves and Their Evolution of the RLW-Burgers Equation, Abstract and Applied Analysis, 2012, 2012, 109235, https://doi.org/10.1155/2012/109235.
[36] F.M. Al-Askar, W.W. Mohammad, M. El-Morshedy, The analytical solutions for stochastic fractional-space Burgers' equation, J. Math. 2022 (2022), 9878885, https://doi.org/10.1155/2022/9878885, 8pages.
[37] F.M. Al-Askar, C. Cesarano, W.W. Mohammad, Multiplicative brownian motion stabilizes the exact stochastic solutions of the Davey–Stewartson equations, Symmetry 14 (2022) 2176, https://doi.org/10.3390/sym14102176.
[38] S. Alshammari, W.W. Mohammad, S.K. Samura, S. Faleh, The analytical solutions for the stochastic-fractional Broer–Kaup equations, Mathematical Probs. Engineering, 2022 (2022), 6895875, https://doi.org/10.1155/2022/6895875, 9pages.
[39] W.W. Mohammad, R. Qahiti, H. Ahmad, J. Baili, F.E. Mansour, M. El-Morshedy, Exact solutions for the system of stochastic equations for the ion sound and Langmuir waves, Results Phys. 30 (2021), 104841, https://doi.org/10.1016/j.rinp.2021.104841.